Published in final edited form as:
Genes Brain Behav. 2012 October ; 11(7): 837–847. doi:10.1111/j.1601-183X.2012.00836.x.

Inactivation of *Pde8b* enhances memory, motor performance, and protects against age-induced motor coordination decay

Li-Chun Lisa Tsai[§], **Guy Chiu-Kai Chan**[§], **Shannon N. Nangle**[§], **Masami Shimizu-Albergine**[§], **Graham Jones**[§,†], **Daniel R. Storm**[§], **Joseph A. Beavo**[§], and **Larry S. Zweifel**[§,†]

[§]Department of Pharmacology, University of Washington, Seattle, Washington 98195, USA

[†]Department of Psychiatry and Behavioral Sciences, University of Washington, Seattle, Washington 98195, USA

Abstract

Phosphodiesterases (PDEs) are critical regulatory enzymes in cyclic nucleotide signaling. PDEs have diverse expression patterns within the central nervous system (CNS), show differing affinities for cyclic adenosine monophosphate (cAMP) and cyclic guanosine monophosphate (cGMP), and regulate a vast array of behaviors. Here, we investigated the expression profile of the PDE8 gene family members *Pde8a* and *Pde8b* in the mouse brain. We find that *Pde8a* expression is largely absent in the CNS; by contrast, *Pde8b* is expressed in select regions of the hippocampus, ventral striatum, and cerebellum. Behavioral analysis of mice with *Pde8b* gene inactivation (PDE8B KO) demonstrate an enhancement in contextual fear, spatial memory, performance in an appetitive instrumental conditioning task, motor-coordination, and have an attenuation of age-induced motor coordination decline. In addition to improvements observed in select behaviors, we find basal anxiety levels to be increased in PDE8B KO mice. These findings indicate that selective antagonism of PDE8B may be an attractive target for enhancement of cognitive and motor functions; however, possible alterations in affective state will need to be weighed against potential therapeutic value.

Introduction

G-protein coupled receptor (GPCR) signaling through $G\alpha_{s/Olf}$ and subsequent stimulation of adenylyl cyclase activity is the canonical means of cAMP accumulation in the mammalian central nervous system (Offermanns 2001). Subsequent cAMP-dependent activation of protein kinase A (PKA) and phosphorylation of proteins, such as the cAMP response-element binding protein (CREB) transcription factor, is a major regulator of synaptic plasticity associated with learning and memory (Poser & Storm 2001). The ubiquitous nature of this second messenger system, linkage to numerous neurological and psychiatric diseases, and diversity in GPCRs coupled to $G\alpha_{s/Olf}$ and adenylyl cyclases has provided fertile ground for the development of targeted therapeutics. In addition to the therapeutic potential of this signaling pathway, pharmacological and genetic gain and loss of function experiments have provided a wealth of knowledge regarding the basic biology and physiology of cAMP signaling cascades in the CNS.

Following stimulated synthesis of cAMP, temporal and spatial control of intracellular cAMP signaling is tightly regulated by cyclic nucleotide hydrolysis through phosphodiesterases

Corresponding author: Larry S. Zweifel, Address: University of Washington, Department of Pharmacology, Box 357380, Seattle, WA 98195-7280, USA, larryz@uw.edu, Tel: 206 685-6155, FAX: 206 685-3822.

The authors have no conflicts of interest to report.

(PDEs) (Conti & Beavo 2007). In mammals, there are 11 families of PDEs, and each PDE family has its own unique kinetic, regulatory partners, as well as inhibitor sensitivity (Bender & Beavo 2006). Of these PDEs, the PDE8 family is one of the more recently discovered. The PDE8 family consists of two distinct genes -*Pde8a* and *Pde8b*. PDE8A and PDE8B have a high affinity for cAMP and hydrolyze cAMP with a low K_m; additionally, neither of the PDE8s can effectively hydrolyze cGMP, nor are they regulated by cGMP (Fisher *et* al. 1998; Soderling *et al.* 1998). Recent studies have indicated potential functions of PDE8B, in thyroid cells (Arnaud-Lopez *et al.* 2008), adrenal cells (Horvath *et al.* 2008; Tsai *et al.*2011), and pancreatic β cells (Dov *et al.*2008); however, little is known about the influence of PDE8s on CNS function.

Like GPCRs and adenyly cyclases, the diversity of PDE families and their distinctive distribution make them attractive therapeutic targets for numerous CNS and peripheral processes. The clinical success of PDE5 selective inhibitors has provided impetus towards the design of therapeutics targeting other PDE families (Levy *et al.* 2011). For example, antagonism of the PDE4 family has been tested for improving cognitive function (Barad *et al.*1998) and PDE10A inhibition has been targeted for the treatment of motor degenerative impairments associated with Huntington's disease (Giampa *et al.* 2010). *Pde8b* expression analysis in humans has demonstrated regionally distributed expression patterns, with the highest levels in the striatum and hippocampal formation (Lakics *et al.* 2010; Perez-Torres *et al.* 2003). Clinically, a mutation in the *Pde8b* gene has been implicated in autosomal-dominant striatal degeneration (ADSD) (Appenzeller *et al.* 2010) and higher levels of *Pde8b* transcript have been observed in the hippocampal dentate gyrus of Alzheimer's patients (Perez-Torres *et al.* 2003).

Although expression and linkage analysis suggest that PDE8B may play an important role in brain function, a thorough behavioral analysis of PDE8B function has not been demonstrated. To better understand PDE8B function in the CNS and to determine the viability of targeted therapeutics towards PDE8B for treatment of neurological disorders, we further investigated the anatomical distribution of *Pde8b* gene expression in the mouse brain, and through targeted gene inactivation investigated the behavioral consequences of loss of PDE8B function.

Methods

Animals

All animal usage and procedures were approved by the Institutional Animal Care and Use Committee of the University of Washington (Seattle, WA) in accordance with the National Institutes of Health Guide for Care and Use of Laboratory Animals. Mice were housed in a 12 hour light-dark cycle and behaviors were performed during the light phase. PDE8B KO were generated as described (Tsai *et al.* 2011). Briefly, gene targeting was performed in ES cells (Cell Line E14; 129P2/OlaHsd; Deltagen, San Mateo, CA) derived from the 129/OlaHsd substrain and subsequently backcrossed to the C57BL/6 strain greater than fifteen generations. All mice for experimentation were obtained through a double $Pde8b^{+/-}$ cross. Male PDE8B KO mice between the ages of 4–12 months (unless otherwise noted) were used in all experiments, and an approximate equal number of age-matched, male wild type (WT) littermates were used as controls. All animals were handled before behavioral testing as follows: Initially, mice were handled in groups along with their cage mates for 10 min per day for 2 days. Subsequently, each mouse was handled individually for 5 min per day for 2 days. Finally, mice were housed individually, and handled twice a day, 5 min per session for 3 additional days. During the handling sessions, petting and rubbing, as well as "catch-and-release" were performed. For experiments in which mice were used in multiple assays, only one stressful paradigm was performed and was always proceeded by a non stressful

procedure. All instances were mice were used in more than one assay are described within the specific methods section. All behavioral experiments were performed with the researchers blind to the genotypes.

β-Gal Activity Staining

Anesthetized animals were perfused with 0.2% heparin-PBS, followed by 4% (w/v) paraformaldehyde in 0.1 M phosphate buffer, pH 7.4. After perfusion, brains were removed from the skull, and postfixed with the same 4% paraformaldehyde solution on ice (6 hr) then rinsed with 10% sucrose-PBS buffer, soaked in 20% (8 hr) and 30% sucrose (overnight) to remove paraformaldehyde and to cryoprotect the tissue. The tissues were then embedded in Tissue-Tek® OCT™ (Sakura Finetek U.S.A, Inc., Torrance, California, USA) then frozen and stored at −80 °C until cryostat sectioning at −20 °C. The 20 μm sagittal sections were mounted onto slides and placed in an X-gal staining mixture (2 mM $MgCl_2$, 0.01% sodium deoxycholate, 0.02% Nonidet P-40, 5 mM EGTA, 20 mM $K_3Fe(CN)_6$, 20 mM $K_4Fe(CN)_6 \bullet H_2O$, and 1 mg/mL X-gal in PBS, pH 7.4) at 37 °C overnight. After X-gal staining, slides were washed three times with PBS, pH 7.4, once with dH_2O, then counterstained with eosin and mounted with Permount® (Thermo Fisher Scientific, Waltham, MA, USA).

Morris water maze

The water maze was a circular feeding trough (79 cm in diameter) filled with 25°C water rendered opaque by the addition of nontoxic white paint. A rectangular escape platform (5 cm × 7.5 cm) was placed 1 cm beneath the water surface at a fixed location throughout the training period. During each training trial, mice were individually released into the maze at a random location near the edge of the pool, and allowed to swim freely until they found and climbed onto the escape platform and remained there for 30 sec. For each case in which an animal was unsuccessful in finding the platform after 90 sec, the animal was placed onto the escape platform and not retrieved until they remained there for 30 sec. The mice received 3 training trials per day with a minimal 30 min break between each trial. After all mice had sufficiently learned the task, determined by their ability to find the platform within 10 sec, a probe test was administered 24 hours after the last conditioning trial. For these experiments a total of n = 13 WT and n = 12 PDE8B KO mice were used. A portion of these mice (n = 7, WT and n = 6, KO) were utilized in a novel object recognition task one week prior to water maze conditioning. During the probe test, the submerged platform was removed and the movement of each individual animal was recorded by a video camera fixed directly above the pool. Video footage was analyzed using Ethovision software (Noldus Information Technology, Leesburg, VA, USA) to determine the number of platform crossings, time spent and frequency of entries into each quadrant. For the remote memory test, mice were trained as above, except that all mice received 4 days of conditioning. A total of 22 mice were used for this experiment (n = 10, WT and n = 12 KO). One PDE8B KO mice failed to escape onto the hidden platform within the allotted time on 10 of 12 trials and was removed from the experiment.

Contextual and delayed cue fear conditioning

Contextual fear conditioning was conducted as previously described (Athos *et al.* 2002). First, the animals were transferred to behavioral testing room at least one week prior to the pre-handling sessions allowing the mice to acclimate. Contextual fear conditioning was performed in a plexiglass chamber with a shock grid floor and a 16″ × 16″ photobeam sensor grid (Truscan Mouse Chamber manufactured by Coulbourn Instruments, Allentown, PA, USA). During day one of the experiment, each mouse was placed in the conditioning chamber individually for 2 min to habituate, then a 0.7 mA foot shock (2 sec) has administrated through the grid floor. After conditioning, mice remained in the cage for an

additional minute to facilitate the association of the shock with the conditioning chamber and were then returned to their home cage. 24 hours later, mice were returned to the same conditioning chamber to determine and the amount of freezing time during a 2 minute re-exposure. Freezing time was scored by hand (sampled every 5 sec) and by computer software based on infrared beam breaks; no difference was detected between the two methods so only computer generated scores are presented. For context-independent freezing following conditioning, mice were treated as above, except that foot shock was delivered in Med Associates ENV-300 chambers (Med Associates, St. Albans, VT, USA), a context distinct from the testing apparatus. For these experiments a total of n = 11 WT and n = 12 PDE8B KO mice were used for contextual conditioning and n = 10 WT and n = 12 PDE8B KO mice were used for context-independent testing. Mice used for context-independent conditioning were previously assayed in the Morris water maze remote memory paradigm one week prior.

Similar to contextual fear conditioning, delayed cued fear conditioning used an adverse stimulus (foot shock) paired with a 90–100dB audio tone. The tone was played during the last 30 sec of the 2 min habituation period followed by delivery of a 2 sec (0.7 mA) foot shock. As in the contextual fear conditioning, the mice remained in the cage for an additional minute to facilitate the pairing between the shock and the tone (as well as the context of the conditioning chamber). 24 hours post-training, freezing behavior was manually scored for 2 min in a novel context (a hexagonal plexiglass cage). For these experiments a total of n = 11 WT and n = 11 PDE8B KO mice were used. A portion of these mice, n = 6 WT and n = 6 PDE8B KO mice had been previously assayed in the Morris water maze, three weeks prior to fear conditioning.

Shock Sensitivity Assay

In this test, naïve animals were placed one at a time into the same plexiglass conditioning chamber as used in contextual fear conditioning. A series of electrical shocks with increasing intensity (from 0.05 mA to 0.7 mA increased in 0.05 mA increments) were delivered to the mice and their reactions were observed. Mice were allowed to freely explore the chamber for 2 min, after which the first electrical shock was delivered through the floor grid for 2 sec. After a 2 min recovery period from the previous shock, a second higher intensity shock was delivered. We classified the general reactions of the mice into 4 categories - flinching, flinching and vocalization, jumping, and jump and vocalization. We evaluated the sensitivity of individual animals to a given current by their reactions. For these experiments a total of n = 3 WT and n = 5 PDE8B KO mice were used.

Elevated plus maze

The elevated plus maze was conducted as described previously (Bruchas *et al.* 2009, Lister 1987). The apparatus was comprised of two open arms ($25 \times 8 \times 12$ cm^2) and two closed arms ($25 \times 8 \times 12$ cm^3) that extended from a common central area 50 cm above the ground (Med Associates, St. Albans, VT, USA). Mice naive to experimental testing were transported to a designated room (low light condition, ≈10–20 lux) one hour prior each experiment to acclimate. During each trial, a mouse was placed in the center of the maze, and allowed to freely explore for 6 min and movement was monitored by video camera. Time spent in the closed arms versus the open arms were scored using Ethovision software (Noldus Information Technology, Leesburg, VA, USA). Lighting was adjusted such that control animals spend approximately equal time in both the open and closed arms. For these experiments a total of n = 5 WT and n = 11 PDE8B KO mice were used.

Open field test

The open field test was performed in a circular arena (49 cm in diameter), evenly illuminated by white overhead fluorescent lighting. The central area (≈17 cm in diameter) was designated as the center zone. Each mouse was placed in this area and left to freely explore for 10 min. We recorded the movement of each mouse using a video camera that was mounted directly above the circular arena. The video footage was analyzed using Ethovision software (Noldus Information Technology, Leesburg, VA, USA). For these experiments a total of n = 6 WT and n = 5 PDE8B KO experimentally naive mice were used.

Instrumental learning

Mice were placed on food restriction for 10–14 days until 85% of the original body weight reached and held steady for at least 3 days. All training and testing were conducted in operant conditioning chambers (ENV-307W, Med Associates, St. Albans, VT, USA). Prior to the start of conditioning, mice were given a 15 min magazine period in which one food pellet was given freely every minute or if either lever was pressed. Mice then underwent a 60 min instrumental conditioning session daily for 7 consecutive days. Two levers were presented during these conditioning session, and each lever press was reinforced with a 20 mg pellet (Bio-Serv, Frenchtown, NJ, USA) and followed by a 6 sec inter-trial interval (ITI) during which the room light turned off and both levers became inactive. The conditioning session ended either after 50 trials were completed or 60 min had elapsed, whichever came first. When animals were able to complete all 50 trials within the 60 min session, the magazine period was reduced to 5 min and eliminated on the next day. A total of n = 13 WT and n = 13 PDE8B KO mice were used. One cohort of mice (n = 7, WT and n = 6, KO) were previously utilized in a novel object recognition task and water maze conditioning task, the second cohort was used previously in the acoustic startle response paradigm described below.

Startle responses and prepulse inhibtion

Sound-attenuated startle chambers (SR-Lab, San Diego Instruments, San Diego, CA, USA) were used to measure startle responses and prepulse inhibition (PPI) as previously described (Zweifel *et al*. 2011). A 65 dB background white noise was maintained throughout the experiment. Following a 5 min habituation period, a series of escalating 40 ms acoustic pulses (null, 80, 90, 100, 105, 100, and 120 dB) were presented to the mice with an ITI of 30 sec. This series was presented ten times for a total of 70 trials. For these experiments a total of n = 6 WT and n = 6 PDE8B KO mice were used. For PPI, mice were given a 10 min habituation period after which they were presented with five 40 ms, 120 dB, pulse-alone trials. Mice were then presented with 50 trials of either a startle pulse-alone, prepulse presentation at either 5, 10 and 15 dB above background (70, 75, 80 dB, repectively), or a null trial in which there was no acoustic stimulus with an average ITI of 15 sec (range, 5–25 sec). A startle trial consisted of a 40 ms, 120 dB pulse of white noise. Prepulse trials consisted of a 20 ms duration prepulse of 70, 75, or 80 dB intensity, which preceded the 40 ms, 120-dB pulse by 100 ms. PPI was calculated for each prepulse level using the following formula: percentage of inhibition = [(average startle response on prepulse trial/average startle response on pulse–alone trial) × 100]. For these experiments a total of n = 8 WT and n = 6 PDE8B KO mice were used.

Rotarod performace

A rotating rod (4 cm in diameter) incrementally accelerated from 4–40 rpm over 2 min (Rotor-rod, San Diego Instruments, San Diego, CA, USA) was used to determine motor coordination. Mice were trained 3 sessions per day with ≈10 min between sessions. Rotarod

performance was measured by latency to fall from or to clasp the rotating rod. For these experiments a total of n = 7 young adult (< 6 months in age) WT, n = 7 young adult, age-matched PDE8B KO mice, and n = 4 aged adult (>2 years in age) WT and n = 7 age-matched PDE8B KO mice were used.

Statistical Analyses

Statistical analysis was performed using GraphPad Prism (GraphPad Software Inc., La Jolla, CA, USA). Repeated measures analysis of variance (ANOVA) was used for multivariate analysis. Student's t-tests were performed using two-tailed distribution.

Results

Pde8b is expressed in an anatomically restricted pattern in the mouse brain

To investigate the distribution of either *Pde8a or Pde8b* gene expression in the mouse brain, we utilized mouse lines in which *Pde8a or Pde8b* are inactivated by replacement of either exon 17 (*Pde8a*) or exons 14 and 15 (*Pde8b*) with a *lacZ* cDNA (Figure 1a and b) (Tsai *et al.* 2011; Vasta *et al.* 2006). Expression of the exogenous *nls-lacZ* allows visualization of β-galactosidase (β-gal) activity under the control of the endogenous *Pde8a or Pde8b* promoter (Tsai *et al.* 2011; Vasta *et al.* 2006). Analysis of β-gal activity on sagittal brain sections from PDE8A KO mice revealed that β-gal expression is largely undetectable in the brains of these mice (Figure 1c). In contrast to PDE8A KO mice, we observed β-gal activity in PDE8B KO mice, with the highest levels of activity in the dentate gyrus and CA1 regions of the hippocampus, the ventral striatum, and the Purkinje cell layer of the cerebellum (Figure 1d). These results consistent with observed *in situ* hybridization analysis reported by the Allen Institute for Brain Science (http://mouse.brain-map.org).

Inactivation of *Pde8b* leads to enhancement of select behaviors

We have previously demonstrated that replacement of exons 14 and 15 of *Pde8b*, which encodes the catalytic domain of PDE8B, with a cDNA encoding *lacz* is sufficient to disrupt functional PDE8B activity (Tsai *et al.* 2011). To determine the behavioral significance of *Pde8b* expression in the brain, we analyzed PDE8B KO mice and WT littermates in a suite of behavioral tasks. We observed that numerous basic behaviors are unaltered by *Pde8b* inactivation (Table 1). However, we did observe selective enhancement of context-dependent fear, spatial memory, performance in an instrumental conditioning task, and motor coordination (summarized below) indicating that some hippocampal-, striatal-, and cerebellar-dependent behaviors are enhanced following *Pde8b* inactivation. These findings are consistent with several of the well-known functions of cAMP signaling in these brain regions.

Contextual and spatial memory is enhanced in PDE8B KO mice

Pde8b appears most highly expressed in the dentate granule cell layer and CA1 pyramidal cell layers of the hippocampus (figure 1b). These hippocampal subdivisions have been demonstrated to be critical in contextual memory recall and spatial pattern separation (Bourtchuladze *et al.* 1994; Rolls & Kesner 2006). Therefore, we assessed whether Pde8B inactivation would alter contextual fear or spatial memory using either contextual fear conditioning paradigm or Morris water maze.

To determine if genetic inactivation of *Pde8b* alters contextual fear conditioning, we assayed freezing behavior in WT control and PDE8B KO mice, as described (Athos et al. 2002). Briefly, mice were conditioned with a single foot shock (0.7 mA, 2 sec) in a novel context and assayed for context-induced freezing 24 hours later in the same context. PDE8B KO mice exhibited an increase in freezing time compared to WT littermate controls (Figure 2A;

t-test, t_{21}=2.24, p<0.05). Increased freezing behavior was not due to altered sensitivity to foot shock (Figure 2b), nor to mobility (data not shown). To determine whether enhanced freezing in PDE8B KO mice is context specific, we monitored freezing behavior in separate cohorts of control and PDE8B KO mice that were conditioned in a context distinct from the testing apparatus. There was no difference between the two groups (WT, 17.58 ± 1.68 vs. KO, 21.61 ± 3.59; t-test, t_{20}=0.93, p=0.18).

To address the specificity of the enhancement in contextual fear conditioning in PDE8B KO mice, we utilized a delayed cue fear-conditioning task which is less dependent on the hippocampus and more dependent upon the amygdala (Phillips & LeDoux 1992). Mice were conditioned with a single pairing of a 30 second auditory cue (90–100 dB) that co-terminated with foot shock (0.7 mA, 2 sec). Cue-evoked freezing was assessed in a context independent of the conditioning chamber 24 hours later. Learning in this task was indistinguishable between PDE8B KO and WT control mice (Figure 2c; t-test, t_{20}=0.37, p=0.36).

Next, we investigated whether functional PDE8B activity might be important in spatial memory using a Morris water maze. Mice were given three training trials per day for 2–3 days to learn the location of a hidden platform. Mice were tested 24 hours following the last conditioning day with the hidden platform removed to assess memory. During training there was no difference between PDE8B KO and control mice in escape latencies, or swim speed (Figure 2d and data not shown; acquisition, two-way repeated measures ANOVA: genotype effect, $F_{1,23}$=1.27, p=0.27; effect of trial, $F_{5,115}$=18.31, p<0.001).

During the probe test, PDE8B KO mice made significantly more entries into the target area (NE quadrant) than controls (Figure 2e; two-way repeated measures ANOVA, genotype X quadrant interaction, $F_{3,69}$=3.28, p<0.05). Increased frequency of entry into the target area was associated with a trend towards increased time spent in the target quadrant; though this measure did not reach statistical significance (Figure 2f; two-way repeated measures ANOVA: genotype X quadrant interaction, $F_{3,69}$=1.52, p=0.22). No differences in the latency to first cross (WT, 22.93 ± 6.59 vs. KO, 19.44 ± 4.42, t-test: t_{23}=0.44, p=0.67) or frequency of crossings (WT, 3.92 ± 0.81 vs. KO, 5.08 ± 0.43, t-test: t_{23}=1.29, p=0.10) of previous platform location were observed.

We next performed a remote memory test on cohorts of mice distinct from those described above. Mice were trained to find the hidden platform as above, except all mice received 4 days of conditioning. Analysis of acquisition revealed a significant effect of trial (Figure 2g; two-way repeated measures ANOVA: trial, $F_{11,198}$=22.01, p<0.001), no genotype effect was detected (two-way repeated measures ANOVA: trial, $F_{1,18}$=2.29, p=0.14). Similar to the probe test performed 1 day following conditioning described above, a probe test 10 days following conditioning revealed a significant genotype x quadrant interaction on the frequency of quadrant entries (Figure 2h, two-way repeated measures ANOVA: genotype x quadrant, $F_{3,57}$=4.22, p<0.01). Again, this increased frequency was associated with a trend towards increased time spent in the target quadrant by PDE8B KO mice (Figure 2i; two-way repeated measures ANOVA: genotype X quadrant interaction, $F_{3,57}$=2.5, p<0.07). No differences in the latency to first cross (WT, 68.20 ± 17.45 vs. KO, 42.39 ± 11.07, t-test: t_{19}=1.27, p=0.10) or frequency of crossings (WT, 4.30 ± 1.42 vs. KO, 7.27 ± 1.76, t-test: t_{19}=1.30, p=0.10) of the previous platform location were observed.

Both PDE8B KO and control mice appeared to take longer to first cross the previous platform location in the remote memory test compared to the 1 day probe test (WT 1 day, 22.93 ± 6.59 vs. WT remote, 68.20 ± 17.45; KO 1 day, 19.44 ± 4.42 vs. KO remote, 42.39 ± 11.07). Statistical analysis across all groups revealed a significant difference in control mice

during the remote memory test compared to the 1 day test, this was not significant in PDE8B KO mice (one-way ANOVA: F_3 =4.62, p<0.01; Bonferroni's Multiple Comparisons test, WT remote vs. WT 1 day, p<0.05 and WT remote vs. KO 1 day, p<0.01).

Appetitive instrumental behavior is enhanced in PDE8B KO mice

Analysis of β-gal activity in PDE8B KO mice demonstrated a high level of enrichment of *Pde8b* expression in the ventral striatum. Because PDEs are important for hydrolysis of cAMP generated in response to dopamine D1 receptors in the striatum and this signaling is important for reward learning and motivated behavior, we hypothesized that appetitive instrumental learning, motivation, or both might be altered in PDE8B KO mice. First, we tested PDE8B KO and WT control mice in a fixed ratio (FR) schedule in which a single lever press resulted in delivery of a reward pellet (FR1). Two levers were activated at the start of each trial signaled by the illumination of the chamber house light. Following a successful trial the house light was turned off, the pellet was dispensed, and the levers where inactivated; six seconds later the house lights were re-illuminated and the levers were re-activated. Both active and inactive lever presses where recorded over 50 trials or for 1 hour, whichever came first. Total lever presses per day did not differ significantly between groups (Figure 3a; two-way repeated measures ANOVA: genotype X day interaction, $F_{6,144}$=0.74, p=0.62); however, there was a trend towards an overall effect of genotype (two-way repeated measures ANOVA: genotype $F_{1,167}$=3.62, p=0.059).

To determine the precision of lever pressing behavior we scored non-rewarded lever presses across days. Analysis of non-rewarded lever presses revealed an overall genotype effect (Figure 3b; two-way repeated measures ANOVA: genotype, $F_{1,167}$=5.55, p=0.02), with PDE8B KO mice making more non-rewarded presses, particularly during the first days of training; however, no significant genotype X day interaction was detected (two-way repeated measures ANOVA: genotype X day interaction, $F_{6,144}$=2.01, p=0.06).

Following the fourth day of training all mice were completing 50 lever presses within the 1 hour time window; moreover, total lever presses and total non-rewarded lever presses were equivalent indicating both groups were equally precise in their performance (Figure 3a and B, days 5–7). Intriguingly, PDE8B KO were faster at completing the task at this later stage compared to control mice (Figure 3c, days 5–7). To elucidate further the extent to which PDE8B KO mice are performing better than control mice we analyzed cumulative reward acquisition on days 5–7. PDE8B KO mice performed significantly better than controls on all three days (Figure 3d-f; two-way repeated measures ANOVA: day 5, genotype X time, $F_{29,725}$=3.47, p<0.0001; day 6, genotype X time, $F_{29,725}$=8.86, p<0.0001; day 7, genotype X time, $F_{29,725}$=5.22, p<0.0001).

To assess whether increased performance in instrumental conditioning by the PDE8B KO mice reflects an enhancement of motivated behavior, we tested PDE8B KO and control mice in a progressive ratio task. Break point analysis, as assessed by the total lever processes in the last trial completed, did not differ between PDE8B KO and control mice (Figure 3g). Finally, to determine whether differences in performance between PDE8B KO and WT mice are due to differences in instrumental learning, we performed a two-lever discrimination task. Mice were given block-training sessions for 6 days to associate a cue light above one of two levers with the active lever. Block trials of 10 light-lever pairings were given on each lever. On day seven mice were assayed for two-lever discrimination based on their ability to discriminate which of the two levers were active; active levers were assigned pseudo randomly. No difference was observed between control and PDE8B KO mice, with both groups performing at or above 80% accuracy (Figure 3h).

Age-induced decay of motor performance is attenuated in PDE8B KO mice

Expression of *Pde8b* in the cerebellum, together with previous observations linking *Pde8b* to ADSD, a progressive motor degenerative disorder, suggests that *Pde8b* inactivation may be associated with altered motor coordination (Appenzeller *et al.* 2010; Perez-Torres *et al.* 2003). To investigate this further, we monitored latency to fall from a rotating rod using an escalating rotarod task in both young (Figure 4a) and aged (Figure 4b) adult mice. Analysis of young adult mice revealed a significant effect of training (two-way repeated measures ANOVA: trial, $F_{8,96}$=8.00, p<0.001), but not genotype (two-way repeated measures ANOVA: genotype, $F_{1,12}$=4.16, p=0.06). In contrast, *Pde8b* inactivation had a significantly increased latency to fall in aged adult mice (two-way repeated measures ANOVA: genotype, $F_{1,8}$=17.91, p=0.003). Analysis of average latency to fall across all groups revealed a significant decrease in performance in aged WT mice compared to young adult mice that was not observed in PDE8B KO mice (Figure 4c, ANOVA, F_3 = 37.42, followed by Bonferroni's Multiple Comparisons Test: WT vs WT aged p<0.01). Additionally, this analysis revealed a significant difference in young adults between WT and PDEB KO mice (Bonferroni's Multiple Comparisons Test: WT vs PDE8B KO p<0.05).

Anxiety-like behavior is increased in PDE8B KO mice

Improved memory in contextual fear conditioning and a spatial learning task, along with improved performance in instrumental conditioning and motor coordination suggests that suppression of PDE8B activity overall improves cognitive and motor abilities. Given that alterations in the accumulation of cAMP are linked to numerous psychiatric disorders and the desire to identify PDEs for targeted therapeutic treatment of mood disorders (Xu et al., 2011), we asked whether genetic inactivation of *Pde8b* is associated with changes in affective state. To address this we monitored anxiety-like behavior using two standard laboratory methods, open field and elevated plus maze. Due to the difficulty in detecting increased anxiety levels in these tests under normal lighting conditions, we utilized low-light testing conditions which result in significantly higher percentages of time spent in the center of the open field arena and the open arms of the elevated plus maze (Bruchas *et al.* 2009). PDE8B KO mice spent significantly less time in the center of the arena than WT controls (Figure 5a; t-test, t_9=2.41, p<0.05). Similarly, PDE8B KO mice spent significantly more time in the closed arms of elevated plus maze than the open arms (Figure 5b), contrary to what was observed in WT control mice (PDE8B KO; closed vs. open arms, t-test, t_8=4.24, p<0.01)).

Alterations in cAMP levels are associated with perturbations of sensory motor gating, such as those measured by prepulse inhibition (PPI) of the acoustic startle reflex, which is a frequent endophenotype of psychiatric disorders such as schizophrenia (Clapcote *et al.* 2007). To determine whether *Pde8b* inactivation alters PPI, we first monitored acoustic startle responses (ASR) across multiple startle pulse intensities to determine whether baseline differences in ASR exist between PDE8B KO and WT control mice. ASR curves between the two groups were indistinguishable (Figure 5c, two-way repeated measures ANOVA: genotype effect, $F_{1,10}$=0.03, p=0.86). To monitor PPI, we measured acoustic startle at 120 dB in the presence or absence of 70, 75, and 80 dB prepulses. No significant differences in PPI between PDE8B KO and WT control mice were detected (Figure 5d, two-way repeated measures ANOVA: genotype effect, $F_{1,12}$=0.02, p=0.89).

Discussion

The present study confirms *Pde8b* expression in the brain and illustrates a regionally restricted enrichment. Consistent with the expression pattern of *Pde8b*, behavioral analysis of mice with genetic inactivation of both *Pde8b* alleles demonstrates: 1) enhanced contextual

fear conditioning; 2) improved spatial memory; 3) increased performance during instrumental appetitive conditioning; 4) attenuation of age-induced motor coordination decline; and 5) increased basal anxiety levels.

Previous analysis of *Pde8b* in humans has demonstrated regionally restricted patterns of expression, with the highest levels in the striatum, hippocampal CA1 and dentate gyrus, cortex, and cerebellum (Lakics *et al.* 2010; Perez-Torres *et al.* 2003). Our findings utilizing a lacZ reporter assay from brain sections of PDE8B KO confirm a similar pattern of expression in mice and are consistent with *in situ* analysis of *Pde8b* expression performed by the Allen Brain Institute for Brain Science (http://mouse.brain-map.org).

Hippocampal-dependent learning and memory, such as contextual fear and spatial pattern recognition, are known to be regulated by cAMP-dependent processes (Poser & Storm 2001; Sweatt 2001). We observed high levels of expression of the *Pde8b* within two major subdivisions of the hippocampus, CA1 and dentate gyrus that are regions critical for memory recall and spatial pattern recognition (Rolls & Kesner 2006). Consistent with the importance of cAMP in hippocampal function and the high level of *Pde8b* expression in these brain regions, we observed that the PDE8B KO mice had significantly enhanced contextual fear and spatial memory. Though these findings are consistent with cAMP signaling in the hippocampus, similar signaling pathways in the ventral striatum are also known to play a role in spatial learning and memory (Ferretti *et al.* 2010); thus, the contribution of inactivation of *Pde8b* in the ventral striatum to enhanced spatial memory reported here cannot be excluded. Similar to the effects of *Pde8b* inactivation of reported here, antagonism of PDE4 and analysis of PDE4D KO mice has have also demonstrated improved performance in several learning paradigms (Li et al. 2011), as well enhance early-phase long-term potentiation (Rutten *et al.* 2008). We have previously demonstrated that PDE8B can act synergistically with PDE4 in other tissues (Tsai *et al.* 2011); thus, it will be interesting to determine if a similar synergy might exist in the hippocampus.

Similar to cAMP signaling in the hippocampus, striatal regulation of cAMP levels downstream of dopamine receptor activation is critical for numerous aspects of motor function, reward learning, and motivated behavior (Nishi *et al.* 2008). We find that *Pde8b* is expressed in the striatum as previously reported; however unlike in the human studies (Perez-Torres *et al.* 2003), we find that expression of *Pde8b* in mice is higher in the ventral striatum compared to the dorsal striatum. Increased performance by PDE8B KO mice in a simple instrumental conditioning task are opposite those reported for PDE10A KO mice (Piccart *et al.* 2011), suggesting that PDE10A and PDE8B may be regulating distinct neuronal populations within the striatum that serve opposing roles, such as the direct and indirect pathway. Interestingly, we find that although the overall performance of PDE8B KO mice is faster than that of WT mice in completing the simple instrumental conditioning task, these mice made more errors (non-rewarded lever presses) during the first days of training. This finding indicates, at least early on in conditioning, faster performance comes at the cost of diminished accuracy. Nonetheless, with further conditioning PDE8B KO mice made as few errors as control mice, yet still completed the task more quickly. Finally, although our data suggests that *Pde8b* in mice is more highly expressed in the ventral as opposed to the dorsal striatum, they do not discount the known importance of the dorsal striatum in performance and learning of simple instrumental responding (Shiflett & Balleine 2011).

A frameshift mutation in *Pde8* that results in loss of PDE8B function has been genetically linked to the autosomal dominant striatal degenerative disorder, ADSD (Appenzeller *et al.* 2010). Although we find that *Pde8b* is expressed in the striatum, loss of PDE8B function in mice does not impair motor performance, even in aged animals. In fact, we find the opposite result. Inactivation of *Pde8b* not only improved motor performance in young adult animals,

it was protective against age-induced decline in motor coordination. Consistent with our rotarod findings we observed that PDE8B KO mice were slightly or even significantly better in tasks that required motor coordination; as evidenced by reduced latencies to find the platform in the Morris water maze and reduced latency to complete the instrumental conditioning task. The reason for these apparently disparate results is not clear; however, one possibility is that we find the highest levels of *Pde8* expression in the ventral striatum and cerebellum in mice, which contrasts with the expression pattern in humans where *Pde8b* appears highest in the dorsal striatum (Appenzeller *et al*. 2010; Lakics *et al*. 2010; Perez-Torres *et al*. 2003).

The potential therapeutic value of developing PDE8B elective inhibitors for treatment of hypothyroidism, Cushing's disease, testosterone deficiency, or cognitive and motor impairments is tempered somewhat by our observation that loss of PDE8B function significantly increases anxiety-like behavior. In addition to our findings, others have demonstrated that increasing cAMP levels either by introducing a constitutively active $G_{\alpha s}$ to the striatum (Favilla *et al*. 2008), by treating animals chronically with a PDE4 inhibitor, rolipram, (Heaslip & Evans 1995; Imaizumi *et al*.1994; Li *et al*. 2009; Silvestre *et al*. 1999), or by genetically inactivating PDE10A is sufficient to trigger anxiety-like behaviors. Given the prevalent nature of findings relating to the anxiogenic properties of attenuating PDE activity, the therapeutic value of PDE antagonism must be weighed against potential alterations in affective state. Due to the robust improvements observed in motor coordination and cognitive function, PDE antagonism coupled with anxiolytic therapies may be a strategy that could circumvent this potential confounding side effect.

Acknowledgments

We would like to thank members of the Zweifel, Beavo, and Storm laboratories and Dr. Ali D. Guler for helpful discussion on this manuscript. This work was supported by grant from the National Institutes of Health. P30MH089887 (LSZ, LLT, SNN, and GLJ). R01GM083926 and R01AR056221 (JAB, LLT, SNN, and MSA). RO1MH073601 (DRS and GCKC).

References

Appenzeller S, Schirmacher A, Halfter H, Baumer S, Pendziwiat M, Timmerman V, De Jonghe P, Fekete K, Stogbauer F, Ludemann P, Hund M, Quabius ES, Ringelstein EB, Kuhlenbaumer G. Autosomal-dominant striatal degeneration is caused by a mutation in the phosphodiesterase 8B gene. Am J Hum Genet. 2010; 86:83–87. [PubMed: 20085714]

Arnaud-Lopez L, Usala G, Ceresini G, Mitchell BD, Pilia MG, Piras MG, Sestu N, Maschio A, Busonero F, Albai G, Dei M, Lai S, Mulas A, Crisponi L, Tanaka T, Bandinelli S, Guralnik JM, Loi A, Balaci L, Sole G, Prinzis A, Mariotti S, Shuldiner AR, Cao A, Schlessinger D, Uda M, Abecasis GR, Nagaraja R, Sanna S, Naitza S. Phosphodiesterase 8B gene variants are associated with serum TSH levels and thyroid function. Am J Hum Genet. 2008; 82:1270–1280. [PubMed: 18514160]

Athos J, Impey S, Pineda VV, Chen X, Storm DR. Hippocampal CRE-mediated gene expression is required for contextual memory formation. Nat Neurosci. 2002; 5:1119–1120. [PubMed: 12368807]

Barad M, Bourtchouladze R, Winder DG, Golan H, Kandel E. Rolipram, a type IV-specific phosphodiesterase inhibitor, facilitates the establishment of long-lasting long-term potentiation and improves memory. Proc Natl Acad Sci U S A. 1998; 95:15020–15025. [PubMed: 9844008]

Bender AT, Beavo JA. Cyclic nucleotide phosphodiesterases: molecular regulation to clinical use. Pharmacol Rev. 2006; 58:488–520. [PubMed: 16968949]

Bourtchuladze R, Frenguelli B, Blendy J, Cioffi D, Schutz G, Silva AJ. Deficient long-term memory in mice with a targeted mutation of the cAMP-responsive element-binding protein. Cell. 1994; 79:59–68. [PubMed: 7923378]

Bruchas MR, Land BB, Lemos JC, Chavkin C. CRF1-R activation of the dynorphin/kappa opioid system in the mouse basolateral amygdala mediates anxiety-like behavior. PLoS One. 2009; 4:e8528. [PubMed: 20052275]

Clapcote SJ, Lipina TV, Millar JK, Mackie S, Christie S, Ogawa F, Lerch JP, Trimble K, Uchiyama M, Sakuraba Y, Kaneda H, Shiroishi T, Houslay MD, Henkelman RM, Sled JG, Gondo Y, Porteous DJ, Roder JC. Behavioral phenotypes of Disc1 missense mutations in mice. Neuron. 2007; 54:387–402. [PubMed: 17481393]

Conti M, Beavo J. Biochemistry and physiology of cyclic nucleotide phosphodiesterases: essential components in cyclic nucleotide signaling. Annu Rev Biochem. 2007; 76:481–511. [PubMed: 17376027]

Dov A, Abramovitch E, Warwar N, Nesher R. Diminished phosphodiesterase-8B potentiates biphasic insulin response to glucose. Endocrinology. 2008; 149:741–748. [PubMed: 17991719]

Favilla C, Abel T, Kelly MP. Chronic Galphas signaling in the striatum increases anxiety-related behaviors independent of developmental effects. J Neurosci. 2008; 28:13952–13956. [PubMed: 19091983]

Ferretti V, Roullet P, Sargolini F, Rinaldi A, Perri V, Del Fabbro M, Costantini VJ, Annese V, Scesa G, De Stefano ME, Oliverio A, Mele A. Ventral striatal plasticity and spatial memory. Proc Natl Acad Sci U S A. 2010; 107:7945–7950. [PubMed: 20351272]

Fisher DA, Smith JF, Pillar JS, St Denis SH, Cheng JB. Isolation and characterization of PDE8A, a novel human cAMP-specific phosphodiesterase. Biochemical and Biophysical Research Communications. 1998; 246:570–577. [PubMed: 9618252]

Giampa C, Laurenti D, Anzilotti S, Bernardi G, Menniti FS, Fusco FR. Inhibition of the striatal specific phosphodiesterase PDE10A ameliorates striatal and cortical pathology in R6/2 mouse model of Huntington's disease. PLoS One. 2010; 5:e13417. [PubMed: 20976216]

Heaslip RJ, Evans DY. Emetic, central nervous system, and pulmonary activities of rolipram in the dog. Eur J Pharmacol. 1995; 286:281–290. [PubMed: 8608790]

Horvath A, Giatzakis C, Tsang K, Greene E, Osorio P, Boikos S, Libe R, Patronas Y, Robinson-White A, Remmers E, Bertherat J, Nesterova M, Stratakis CA. A cAMP-specific phosphodiesterase (PDE8B) that is mutated in adrenal hyperplasia is expressed widely in human and mouse tissues: a novel PDE8B isoform in human adrenal cortex. Eur J Hum Genet. 2008; 16:1245–1253. [PubMed: 18431404]

Imaizumi M, Miyazaki S, Onodera K. Effects of a non-xanthine adenosine antagonist, CGS 15943, and a phosphodiesterase inhibitor, Ro 20-1724, in a light/dark test in mice. Methods Find Exp Clin Pharmacol. 1994; 16:717–721. [PubMed: 7723470]

Lakics V, Karran EH, Boess FG. Quantitative comparison of phosphodiesterase mRNA distribution in human brain and peripheral tissues. Neuropharmacology. 2010; 59:367–374. [PubMed: 20493887]

Levy I, Horvath A, Azevedo M, de Alexandre RB, Stratakis CA. Phosphodiesterase function and endocrine cells: links to human disease and roles in tumor development and treatment. Curr Opin Pharmacol. 2011; 11:689–697. [PubMed: 22047791]

Li YF, Cheng YF, Huang Y, Conti M, Wilson SP, O'Donnell JM, Zhang HT. Phosphodiesterase-4D knock-out and RNA interference-mediated knock-down enhance memory and increase hippocampal neurogenesis via increased cAMP signaling. J Neurosci. 2011; 31:172–183. [PubMed: 21209202]

Li YF, Huang Y, Amsdell SL, Xiao L, O'Donnell JM, Zhang HT. Antidepressant- and anxiolytic-like effects of the phosphodiesterase-4 inhibitor rolipram on behavior depend on cyclic AMP response element binding protein-mediated neurogenesis in the hippocampus. Neuropsychopharmacology. 2009; 34:2404–2419. [PubMed: 19516250]

Lister RG. The use of a plus-maze to measure anxiety in the mouse. Psychopharmacology (Berl). 1987; 92:180–185. [PubMed: 3110839]

Nishi A, Kuroiwa M, Miller DB, O'Callaghan JP, Bateup HS, Shuto T, Sotogaku N, Fukuda T, Heintz N, Greengard P, Snyder GL. Distinct roles of PDE4 and PDE10A in the regulation of cAMP/PKA signaling in the striatum. J Neurosci. 2008; 28:10460–10471. [PubMed: 18923023]

Offermanns S. In vivo functions of heterotrimeric G-proteins: studies in Galpha-deficient mice. Oncogene. 2001; 20:1635–1642. [PubMed: 11313911]

Perez-Torres S, Cortes R, Tolnay M, Probst A, Palacios JM, Mengod G. Alterations on phosphodiesterase type 7 and 8 isozyme mRNA expression in Alzheimer's disease brains examined by in situ hybridization. Exp Neurol. 2003; 182:322–334. [PubMed: 12895443]

Phillips RG, LeDoux JE. Differential contribution of amygdala and hippocampus to cued and contextual fear conditioning. Behav Neurosci. 1992; 106:274–285. [PubMed: 1590953]

Piccart E, Gantois I, Laeremans A, de Hoogt R, Meert T, Vanhoof G, Arckens L, D'Hooge R. Impaired appetitively as well as aversively motivated behaviors and learning in PDE10A-deficient mice suggest a role for striatal signaling in evaluative salience attribution. Neurobiol Learn Mem. 2011; 95:260–269. [PubMed: 21130175]

Poser S, Storm DR. Role of Ca2+-stimulated adenylyl cyclases in LTP and memory formation. Int J Dev Neurosci. 2001; 19:387–394. [PubMed: 11378299]

Rolls ET, Kesner RP. A computational theory of hippocampal function, and empirical tests of the theory. Prog Neurobiol. 2006; 79:1–48. [PubMed: 16781044]

Rutten K, Misner DL, Works M, Blokland A, Novak TJ, Santarelli L, Wallace TL. Enhanced long-term potentiation and impaired learning in phosphodiesterase 4D-knockout (PDE4D) mice. Eur J Neurosci. 2008; 28:625–632. [PubMed: 18702734]

Shiflett MW, Balleine BW. Molecular substrates of action control in cortico-striatal circuits. Prog Neurobiol. 2011; 95:1–13. [PubMed: 21704115]

Silvestre JS, Fernandez AG, Palacios JM. Effects of rolipram on the elevated plus-maze test in rats: a preliminary study. J Psychopharmacol. 1999; 13:274–277. [PubMed: 10512083]

Soderling SH, Bayuga SJ, Beavo JA. Cloning and characterization of a cAMP-specific cyclic nucleotide phosphodiesterase. Proc Natl Acad Sci U S A. 1998; 95:8991–8996. [PubMed: 9671792]

Sweatt JD. The neuronal MAP kinase cascade: a biochemical signal integration system subserving synaptic plasticity and memory. J Neurochem. 2001; 76:1–10. [PubMed: 11145972]

Tsai LC, Shimizu-Albergine M, Beavo JA. The high-affinity cAMP-specific phosphodiesterase 8B controls steroidogenesis in the mouse adrenal gland. Mol Pharmacol. 2011; 79:639–648. [PubMed: 21187369]

Vasta V, Shimizu-Albergine M, Beavo JA. Modulation of Leydig cell function by cyclic nucleotide phosphodiesterase 8A. Proc Natl Acad Sci U S A. 2006; 103:19925–19930. [PubMed: 17172443]

Xu Y, Zhang HT, O'Donnell JM. Phosphodiesterases in the central nervous system: implications in mood and cognitive disorders. Handb Exp Pharmacol. 2011:447–485. [PubMed: 21695652]

Zweifel LS, Fadok JP, Argilli E, Garelick MG, Jones GL, Dickerson TM, Allen JM, Mizumori SJ, Bonci A, Palmiter RD. Activation of dopamine neurons is critical for aversive conditioning and prevention of generalized anxiety. Nat Neurosci. 2011; 14:620–626. [PubMed: 21499253]

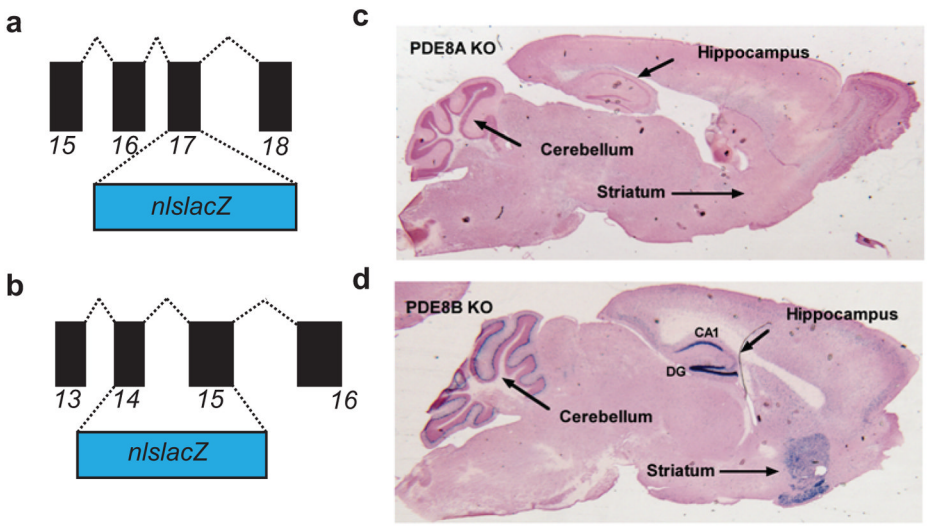

Figure 1. *Pde8b*, but not *Pde8A* expression is enriched in specific brain regions

(a,b) Targeting strategy for selective expression of *lacZ* from endogenous *Pde8a* (a) or *Pde8b* (b) loci and functional gene inactivation in mice (see Vasta et al., 2006 and Tsai et al., 2011 for additional details). (c) Analysis of β-gal activity in PDE8A KO mice reveals *Pde8a* expression is largely undetectable in the mouse brain. (d) Similar analysis of PDE8B KO mice demonstrates regionally restricted enrichment of *Pde8b* expression in hippocampus (CA1 and DG fields), cerebellum, and ventral striatum.

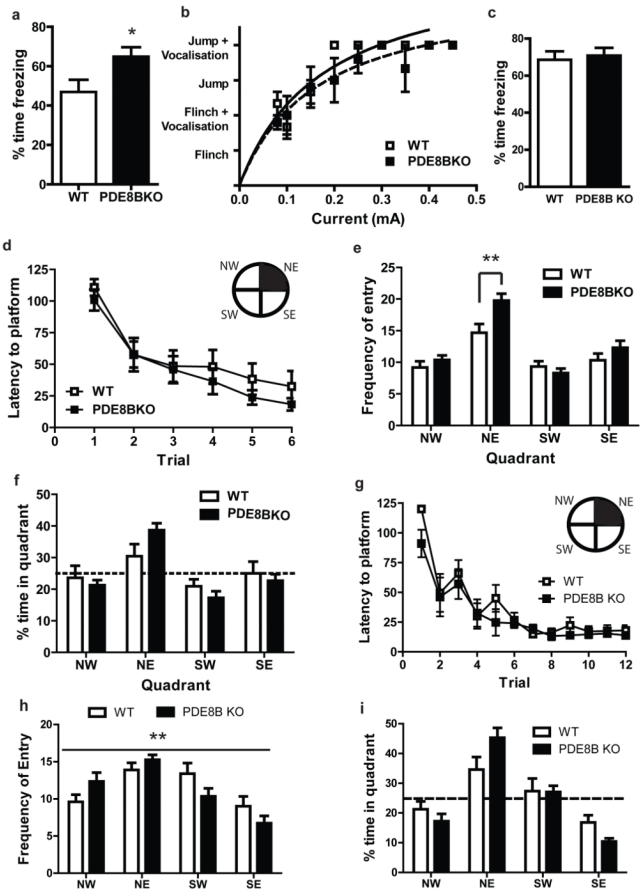

Figure 2. Contextual and spatial memoty is enhanced in PDE8B KO relative to WT mice

(a) Percent time spent freezing in fear-conditioned context is significantly enhanced PDEB KO mice compared to WT controls (PDE8B KO, n = 11; WT, n = 12; *p<0.05). (b) Shock responses to increasing shock amplitude does not differ between PDE8B KO and WT mice (PDE8B, KO, n = 5; WT, n = 3). (c) Percent time freezing in response to the conditioned cue in a novel context following delayed-cue fear conditioning is not different between genotypes (PDE8B, KO n = 11; WT, n = 11). (d) Both PDE8B KO and WT mice showed significant improvement in the acquisition phase of the water maze, as measured by escape latency (PDE8B KO, n = 13; WT, n = 12; p<0.001); inset represents water maze with target quadrant (NE) filled. (e) PDE8B KO mice had significantly more entries into the target quadrant (NE) than WT mice during the probe trial (**p<0.01). (f) Time spent in the target quadrant did not differ between genotypes, though there was a trend towards increased time in the target quadrant for PDE8B KO compared to WT mice. (g) PDE8B KO and WT mice showed significant improvement in the acquisition phase of the water maze for the remote memory test, as measured by escape latency (PDE8B KO, n = 11; WT, n = 10; p<0.001); inset represents water maze with target quadrant (NE) filled. (h) Frequency of entries into the target quadrant, a significant interaction between genotype and quadrant was observed (**p<0.01). (i) Time spent in the target quadrant did not differ between genotypes (p<0.07), a significant effect of quadrant was observed (p<0.001).

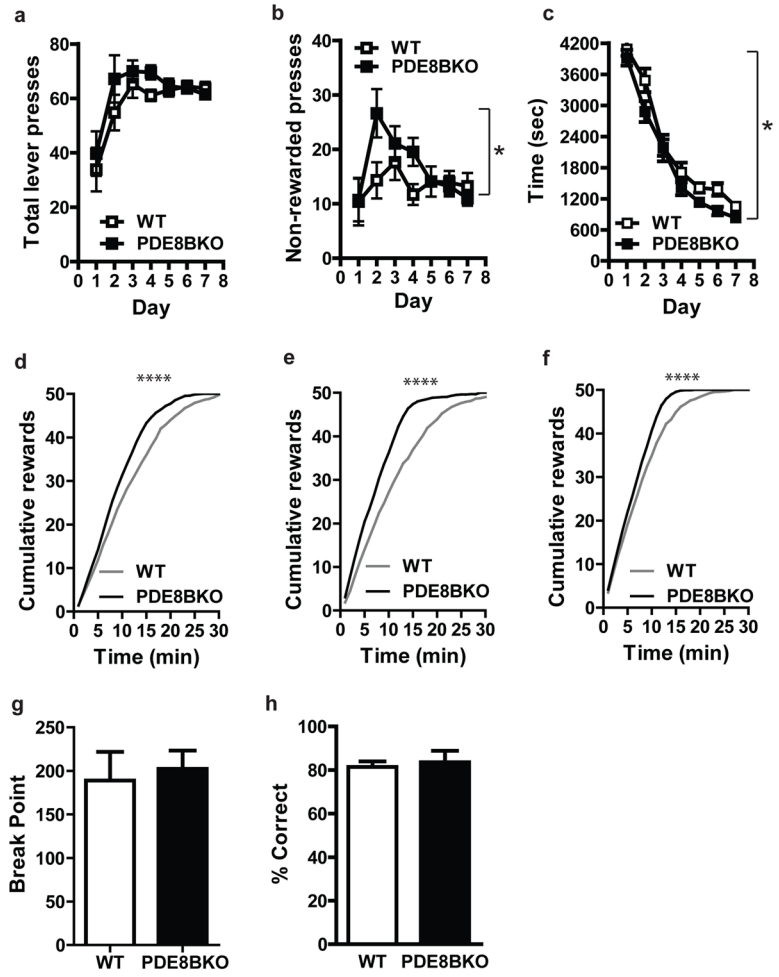

Figure 3. PDE8B KO mice have better performance in a simple instrumental conditioning task than WT mice

(a)Total lever presses (rewarded+ non-rewarded) increased significantly in both PDE8B KO and WT with repeated conditioning in an FR1 reinforcement schedule (PDE8B KO, n = 13; WT n = 13; day effect $p<0.001$). (b) Errant (non-rewarded) lever presses were significantly increased in PDE8B KO mice, most notably during the first few days of conditioning (genotype effect *$p<0.05$). (c) PDE8B KO mice were overall faster at completing 50 rewarded lever presses than WT mice (genotype effect *$p<0.05$). (d–f) Cumulative lever presses over time on the days without pre-conditioning magazine training (days 5 (d), 6(e), and 7(f)) was significantly shorter in PDE8B KO mice compared to WT mice (genotype x time interaction ****$p<0.0001$). (g) Breakpoint analysis on a progressive ratio schedule was not different between genotypes (PDE8B KO, n = 6; WT n = 6). (h) PDE8B KO and WT mice performed similarly in a two-lever discrimination task (PDE8B KO, n = 7; WT n = 7).

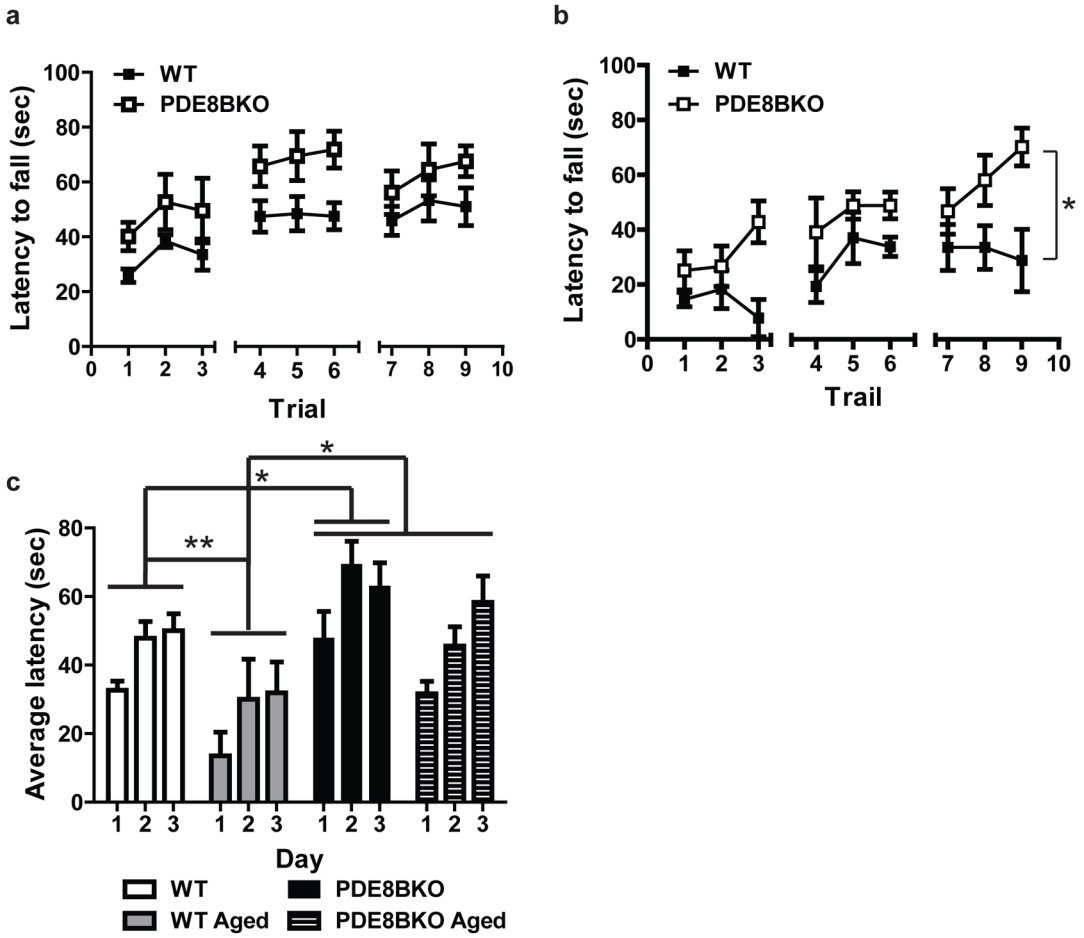

Figure 4. Age-induced decline in rotarod performance is abrogated in PDE8B KO mice compared to WT mice

(a) Latency to fall in the rotarod task increased with conditioning in young mice regardless of genotype (PDE8B KO n = 7, WT n = 7; trial effect $p<0.001$); PDE8B KO mice showed a trend towards increased performance (genotype effect $p=0.056$). (b) Performance of aged mice (>2 yrs old) in the rotarod task also improved with conditioning regardless of genotype (PDE8B KO n = 6, WT n = 4; trial effect $p<0.001$); PDE8B KO mice demonstrated an overall better performance than WT mice (*$p<0.01$). (c) Average latency to fall across days was reduced in aged WT mice compared to all other groups (**$p<0.01$ WT aged vs. WT, *$p<0.05$ WT aged vs PDE8B KO, WT aged vs PDE8B KO aged). In addition, this analysis revealed significant differences between young PDE8B KO mice and young WT mice ($p<0.05$).

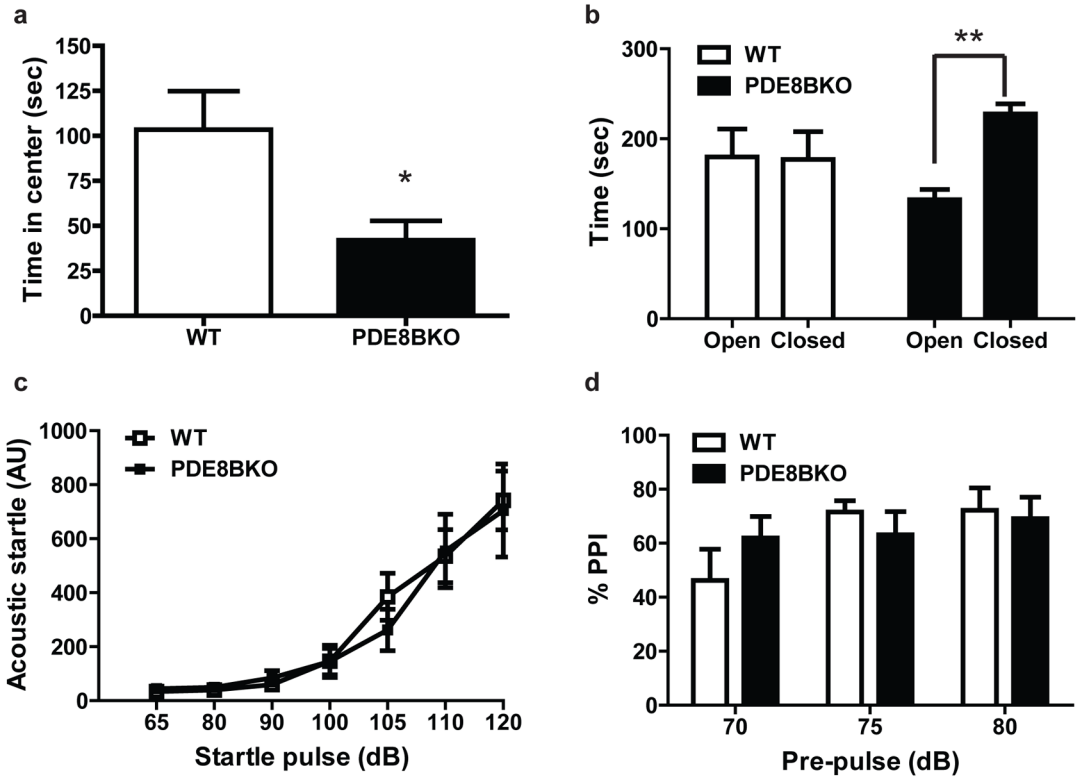

Figure 5. PDE8B KO mice have increased basal anxiety levels compared to WT mice, but do not display alterations in sensory-motor gating as assessed by acoustic startle and PPI

(a) PDE8B KO mice spent significantly less time in the center of an open field (PDE8B KO n = 5, WT n = 6; *p<0.05). (b) PDE8B KO mice spent less time in the open arms of an elevated plus maze compared to the closed arms (PDE8B KO n = 11, WT n = 5; *p<0.05). Acoustic startle in responses in both PDE8B KO and WT mice increased in response to increasing startle pulse intensities (PDE8B KO n = 6, WT n = 6; p<0.001). (d) PPI in response to increasing pre-pulse intensities is not different between PDE8B KO(n = 6) and WT (n = 8) mice.

Table 1
Summary of behavioral analysis of PDE8B KO mice

Phenotypic analysis of PDE8B KO mice compared to WT littermate controls reveals enhancement of performance in several behavioral tasks. However, numerous behaviors are not significantly altered in the absence of functional *Pde8b* expression

Body weight	↔
Locomotor activity	↔
Rotarod	↑
Novel object recognition	↔
Spatial memory	↑
Contextual fear memory	↑
Cued fear memory	↔
Acoustic startle	↔
Fear-potentiated startle	↔
Prepulse inhibition	↔
Instrumental conditioning	↑
Progressive ratio	↔
2-lever discrimination	↔
Elevated-plus maze	↓
Open field	↓

(↔ no change, ↓ decreased relative to WT, ↑ improved performance compared to WT).